einstein
Official Publication of the Instituto Israelita de Ensino e Pesquisa Albert Einstein

ORIGINAL ARTICLE

Exploring the relationship between cognitive performance and magnetic resonance imaging diffusion parameters in elderly individuals

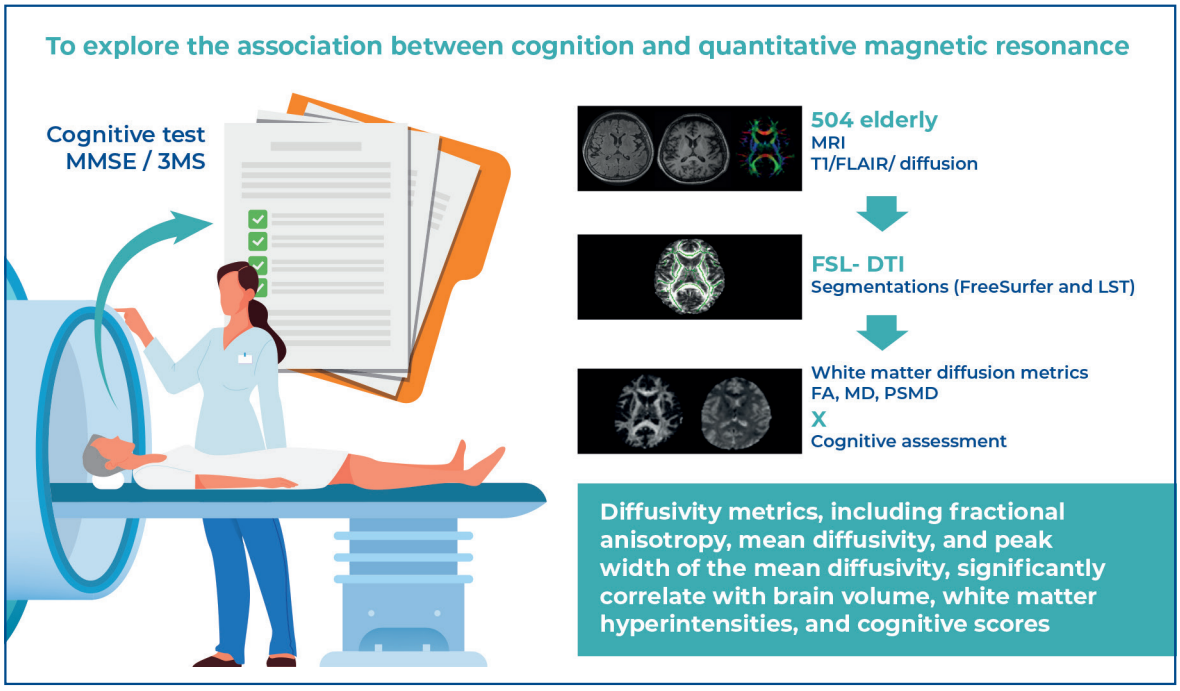

Authors

Mariana Athaniel Silva Rodrigues, Thiago Pereira Rodrigues, Aurea Beatriz Martins Bach, Artur José Marques Paulo, Michel Satya Nasvlasky, Yeda Aparecida de Oliveira Duarte, Mayana Zatz, Edson Amaro Junior

Correspondence

E-mail: mariathaniel@gmail.com

DOI

DOI: 10.31744/einstein_journal/2025AO1467

In Brief

This study investigates the relationship between cognitive performance and brain magnetic resonance imaging diffusion parameters in 504 older adults from São Paulo, Brazil. Using advanced magnetic resonance imaging techniques and cognitive assessments (MMSE and 3MS), the study found significant correlations between diffusivity metrics (fractional anisotropy, mean diffusivity, and peak width of skeletonized mean diffusivity) and brain volume, white matter hyperintensities, and cognitive scores. Findings were validated by comparing them with a UK Biobank cohort. The results suggest that magnetic resonance imaging metrics may be useful imaging markers for monitoring cognitive decline and dementia.

Highlights

- First study to investigate associations between cognitive performance and brain magnetic resonance imaging parameters in an older Brazilian population.
- Uses advanced magnetic resonance imaging diffusion tensor imaging and automated analysis to quantify brain changes.
- Validates findings through comparison with data from a large UK-based cohort.
- Focuses on region-specific assessments, such as the superior longitudinal fasciculus and other key brain areas related to cognition.
- Demonstrates significant correlation between 3MS and MMSE cognitive scores and diffusion metrics, highlighting the role of white matter integrity in cognitive aging.

How to cite this article:

Rodrigues MA, Rodrigues TP, Bach AB, Paulo AJ, Nasvlasky MS, Duarte YA, et al. Exploring the relationship between cognitive performance and magnetic resonance imaging diffusion parameters in elderly individuals. einstein (São Paulo). 2024;22:eAO1467.

einstein
Official Publication of the Instituto Israelita de Ensino e Pesquisa Albert Einstein

e-ISSN: 2317-6385

ORIGINAL ARTICLE

Exploring the relationship between cognitive performance and magnetic resonance imaging diffusion parameters in elderly individuals

Mariana Athaniel Silva Rodrigues[1], Thiago Pereira Rodrigues[2], Aurea Beatriz Martins Bach[3], Artur José Marques Paulo[1], Michel Satya Nasvlasky[4], Yeda Aparecida de Oliveira Duarte[4], Mayana Zatz[4], Edson Amaro Junior[1]

[1] Hospital Israelita Albert Einstein, São Paulo, SP, Brazil.
[2] Hospital São Paulo, Universidade Federal de São Paulo, São Paulo, SP, Brazil.
[3] Oxford University, Oxford, United Kingdom.
[4] Universidade de São Paulo, São Paulo, SP, Brazil.

DOI: 10.31744/einstein_journal/2024AO1467

ABSTRACT

Objective: This study evaluated the association between cognitive function and quantitative magnetic resonance imaging analyses, including brain volume, white matter hyperintensity volume, and diffusivity metrics. **Methods:** This retrospective analysis included 504 older adults from São Paulo, Brazil, who underwent 3T magnetic resonance imaging scans. Image analysis was performed using the FMRIB Software Library (FSL), with peak width of mean diffusivity assessed via a public script. FLAIR signal changes were quantified using the Lesion Segmentation Tool and Fazekas scale. Cognitive performance was assessed using MMSE and 3MS tests. Multiple linear regression, adjusting for control variables, was used to evaluate the relationships between magnetic resonance imaging measurements and cognitive scores, validated against a UK Biobank sample. **Results:** Magnetic resonance imaging demonstrated strong correlations with UK Biobank dataset. Fractional anisotropy, mean diffusivity, and peak width of the mean diffusivity values were significantly associated with white matter hyperintensities (Spearman's rho: -0.630, 0.750, and 0.747, $p<0.001$). Specific brain regions demonstrated strong links between fractional anisotropy and mean diffusivity values and cognitive performance. Fractional anisotropy findings correlated positively with neuropsychological scores ($r=0.315$ for 3MS and $r=0.285$ for MMSE, $p<0.001$). **Conclusion:** Diffusivity metrics, including fractional anisotropy, mean diffusivity, and peak width of the mean diffusivity significantly correlated with brain volume, white matter hyperintensities, and cognitive scores. These findings may serve as potential imaging markers for monitoring cognitive decline and dementia.

Keywords: Diffusion tensor imaging; Cognition; Cognitive dysfunction; Dementia; Neuroimaging; Neuropsychological tests; Aged; Magnetic resonance imaging

INTRODUCTION

Despite medical advances and numerous efforts to mitigate cognitive decline, aging remains a universal process affecting all individuals.[1] Cognitive decline complexity in the older population results from the interplay of various aging-related factors, including cellular senescence, epigenetic modifications, and metabolic dysfunction. Brain aging phenotypes, such as vascular dysfunction, inflammation, and lipid dysregulation, further interact with central nervous system processes, leading to morphological, cognitive, and neuropathological changes, ultimately contributing to neurodegenerative diseases.[2]

How to cite this article:
Rodrigues MA, Rodrigues TP, Bach AB, Paulo AJ, Nasvlasky MS, Duarte YA, et al. Exploring the relationship between cognitive performance and magnetic resonance imaging diffusion parameters in elderly individuals. einstein (São Paulo). 2024;22:eAO1467.

Associate Editor:
Maysa Seabra Cendoroglo
Universidade Federal de São Paulo, São Paulo, SP, Brazil
ORCID: https://orcid.org/0000-0003-2548-2619

Corresponding author:
Mariana Athaniel Silva Rodrigues
Avenida Albert Einstein, 627/701 Morumbi
Zip code: 05652-900 - São Paulo, SP, Brazil
Phone: (55 11) 98416-7338
E-mail: mariathaniel@gmail.com

Received on:
Oct 17, 2024

Accepted on:
May 13, 2025

Conflict of interest:
none.

Dementia, characterized by severe cognitive decline that interferes with daily activities, is most commonly associated with Alzheimer's disease as the leading cause,[3] followed by cerebrovascular disease as the second most common cause.[4]

Particularly, neuroimaging studies on dementia are scarce in low and middle-income countries. This is relevant considering countries such as Brazil have the highest dementia burden and potential for reduced prevalence through addressing seven modifiable risk factors (low education, physical inactivity, midlife hypertension, midlife obesity, depression, smoking, and diabetes mellitus).[5] Despite rising prevalence owing to increased life expectancy, public health investment services remain insufficient.[6]

Cognitive tests, particularly the widely validated Mini Mental State Examination (MMSE), are essential for assessing cognitive function, particularly in the older population, both internationally and in Brazil.[7]

Magnetic resonance imaging (MRI) serves as a valuable *in vivo* marker for nervous system characterization. High-resolution MRI allows for comparative intervention analyses, risk factor control, and central nervous system impact evaluation.[8] However, access to more advanced MRI modalities is challenging in low-middle income countries. When available, advanced MR techniques and analysis methods enables assessment of tissue microstructure organization in these populations. Among these techniques, diffusion tensor imaging (DTI) analyzes water molecule mobility along white matter tracts, revealing white matter molecular properties under physiologic and altered conditions.[9] One of its parameters, fractional anisotropy (FA) is sensitive to microstructural changes, with experimental tests demonstrating a strong correlation with axon number and constitution.[10]

Fractional anisotropy and mean diffusivity (MD) are DTI parameters that demonstrate good intra-scanner reproducibility, and our sample presents ideal data on which all tests were performed with the same equipment and protocol.[11] Peak width of skeletonized mean diffusivity (PSMD) is a newer automated DTI marker quantifying damage related to small vessel disease; however, possible inconsistent results may be found and special care must be taken with quality assessment for motion and distortion artifacts.[12,13]

OBJECTIVE

This study aims to explore the association between cognition and quantitative magnetic resonance imaging analysis, including brain volume, white matter hyperintensity volume, and diffusivity metrics. To ensure external validation and reproducibility, differences among diffusion metrics were compared in two different diffusion magnetic resonance imaging acquisitions in a distinct population, considering the extraordinary sample of older individuals in large population-based studies (UK Biobank and OCTAGENE).

METHODS

Our data is part of the SABE multicenter study coordinated by the Pan American Health Organization developed in urban centers to profile living and health conditions of older adults. In Brazil, the study was conducted in São Paulo with a probabilistic cohort of individuals >60 years old. A comprehensive questionnaire, including health status, housing conditions, work history, and income were reported, alongside functional tests and blood collections for biochemical, immunological, and genetic variables. These were reported by Naslavsky et. al., and detailed in previous methodologic, genetic, and brain matter volumetric evaluation studies.[14-16]

As part of SABE, we analyzed the OCTAGENE study, including a retrospective sample of this population who underwent brain magnetic resonance imaging in 3T equipment (TIM TRIO; Siemens Healthcare, Erlangen, Germany). The imaging followed the same study protocol: T1-weighted volumetric magnetization-prepared rapid-acquisition gradient echo imaging with 1 mm isotropic voxels, 2500ms repetition time, 3.45ms echo time, 1100ms inversion time, and a 7° flip angle. FLAIR isotropic and DTI with 30 directions were also required. Four trained neuroradiologists analyzed images to exclude abnormalities and movement artifacts.[15]

UK Biobank MRI acquisition was performed using similar study protocols,including diffusion MRI and volumetric isotropic T1 MPRAGE and T2 Flair, as detailed in table 1. A standardized six-week training program and routine phantom measurements using UK Biobank MRI scanners ensured harmonized imaging data. Acquisition parameters are displayed table 1.

Images were evaluated by a certified radiologist with specific training in neuroradiology. Substantial structural abnormalities were considered and qualitative evaluation was performed using the periventricular white matter Fazekas scale[17] (score 0, I, II or III). Qualitative data were supported using automated quantification processing tools, including the lesion segmentation tool (LST) toolbox (LGA, Lesion Growth Algorithm)[18] and FreeSurfer software (version 5.3.0;

Table 1. MRI acquisition parameters of T1, T2, and diffusion images according to duration, resolution matrix, and other parameters in OCTAGENE and the UK Biobank protocol

Modality	T1 MPRAGE	T2 FLAIR	Diffusion MRI
Duration, UK Biobank (mins)	4:54	5:52	7:08
Duration, OCTAGENE (mins)	4:23	4:40	3:22
Resolution, UK Biobank	1.0 × 1.0 × 1.0	1.0 × 1.0 × 1.05	2.0 × 2.0 × 2.0
Resolution, OCTAGENE	1.0 × 1.0 × 1.0	0.5 × 0.5 × 1.0	2.2 × 2.2 × 2.2
Matrix, UK Biobank	256 × 256 × 208	256 × 256 × 192	104 × 104 ×72
Matrix- OCTAGENE	256 × 256 × 138	256 × 256 × 160	280 × 280 × 128
Other parameters, UK Biobank	TE/TR=2.01/2000ms, TI=880ms	TE/TR=395/5000ms, TI=1800ms	TR=3600ms, 50 directions/shell, b=0,1000, 2000 s/mm^2, 51 deg, MB=3
Other parameters, OCTAGENE	TE/TR=3.48/2500ms, TI=1000ms	TE/TR=280/5000ms, TI=1800ms	TR=5900, 30 directions/shell, b=0,1000 s/mm^2, 0 deg., MB=2

MRI: magnetic resonance imaging.:

Athinoula A. Martinos Center for Biomedical Imaging, Massachusetts General Hospital, Boston, MA, USA). Processing was performed on a high-performance computer to build models of the cortical surface Results were verified via quality control assessment.[19]

White matter hyperintensities were categorized via periventricular region more related to vascular disease. Classification levels were 0, I, II, and III (0 for single punctate white matter hyperintensities, I for multiple punctate white matter, II for some lesion confluency, and III for large confluent lesions).[17]

Structural image evaluation was performed and statistically controlled in correlation with demographic data (age, years of education, and sex), diffusion metrics (FA, MD, and PSMD), and cognitive tests (MMSE and 3MS).[20-22]

The images were initially evaluated for the technical acquisition quality, excluding cases with incomplete images, unavailable DTI images, and artifacts that could impede analysis.

Diffusivity parameters were considered individually and group analysis was performed with the FMRIB Software library, including validated protocols. The Brain Extraction Tool was used for extracting brain volumes. The "eddy" function from FDT (Diffusion Toolbox) corrected distortions, movement artifacts, and Eddy currents. The DTIFIT command provided FA and MD values. Tract based spatial statistics (TBSS) was used for group assessment.[22] Tract based spatial statistics pipeline was applied to skeletonized data as reviewed by Baykara et al.[23]

Images were processed and analyzed with the FreeSurfer software on a high-performance computer to construct models of the cortical surface.

Statistical analyses

Analyses were performed by a statistician experienced in health data using the IBM SPSS Statistics software package for Windows, Version 20.0, Armonk, NY: IMB Corp., 2011. Bonferroni correction mitigated multiple variable corrections.

Spearman's rank correlation quantified relationships, where coefficients (rho) of 0.1, 0.3, and 0.5 indicate small, medium, and large effects, respectively.[24] Spearman's correlation was applied to assess associations between white matter lesion volume and count, FA, MD, cognitive scores (3MS and MMSE), Fazekas scale scores, and age.

Multiple linear correlation regarded MMSE and 3MS as dependent variables in the model, considering sex, age, and years of education in each of the regions of interest (white matter tracts).

Cluster (groups of contiguous voxels that exhibit similar properties) comparisons of white matter hyperintensity and volume observed in FLAIR images between sexes in relation to FA, MD, and PSMD were performed using the Mann-Whitney test.

A comparison of diffusion metrics (FA, MD, and PSMD) was performed based on outcomes, categorizing scores into MMSE ≤17, severe cognitive impairment[25] and MMSE ≥23, and mild cognitive impairment.[26] Receiver Operating Characteristic (ROC) curves and areas under the curve (AUC) with confidence intervals >95% were employed for this assessment.

A significance threshold of 5% was adhered to for all statistical inferences and tests.

RESULTS

In total, 529 patients underwent MRI, and 504 were selected for analysis. Twenty-five patients (4%) were excluded owing to DTI sequence unavailability or poor image quality.

The studied population had a mean age of 74±9 years, with 326 females (64.6%), an MMSE average score of 25.4, and a standard deviation of ±4.5, out of a total of 30 points (Table 2).

Table 2. OCTAGENE demographic data

	n (%)
Age, (Mean)	504 74±9 years
Sex	
Female	326 (64.6)
Male	178 (35.3)
Cognitive test, (Mean)	
MMSE	25±4.5
3MS	81.7±14.4
Brain volume	956±109 mL
Intracranial volume	1342±226 mL

The 3MS had a mean of 81.7 and standard deviation of 14.4, out of a total of 100 points.

The mean brain volume was 956 mL, with a median of 956 mL, and a standard deviation of 109 mL. The mean intracranial volume in the studied population was 1,342 mL, with standard deviation of 226 mL. The ratio between brain volume and intracranial volume had a mean of 0.72, and a standard deviation of 0.11.

Strong correlations were observed when evaluating lesion volumes and diffusion measures, highlighting volumetric measures and DTI sensitivity (DTI metrics in characterizing white matter abnormalities). The observed correlation coefficients ranged 0.514-0.750 when evaluating lesion volumes alongside diffusion metrics, indicating a robust relationship between these factors (Figure 1).

The global fractional anisotropy values for study participants had a mean of 0.42, with a median of 0.43 and standard deviation of 0.021.

Mean diffusivity analysis among participants had an average value of 0.916, with a median of 0.907, and standard deviation of 0.068.

The global PSMD variable had a median value of 0.30 × 10^{-4} mm^2/s among study participants, with a standard deviation of 0.068.

An exploratory analysis was conducted on all tracts from the JHU White-Matter Tractography Atlas, considering region of interest (ROI) analysis standardized using the FLS software. A multivariate analysis of these regions of interest was performed, considering sex, age, and years of education. The superior longitudinal fasciculus, inferior fronto-occipital fasciculus, and the cingulum gyrus showed the strongest associations with MMSE and 3MS scores (Tables 3 and 4).

A comparative analysis of diffusion metrics (FA, MD, and PSMD) were performed for MMSE ≤17 (MMSE17) and MMSE ≤23 (MMSE23). ROC curvers showed an AUC >0.769 for MMSE ≤17 and AUC >0.625 for the MMSE23 cutoff (Figures 2 and 3).

In a complementary analysis, data from individuals in the UK Biobank were subsampled to evaluate possible variations related to age group differences. The original sample included individuals with a minimum age of 45 years and a maximum of 75. To adjust the samples, the minimum age of 60 years was used as the cutoff (older population), and the maximum age was equal to that of the UK Biobank study (75 years) (Table 5).

Mean FA and MD curves across tracts showed better alignment between OCTAGENE and UK Biobank in the 60-75 years subsample (Figure 4).

The proportional difference formula: (OCT − UK) / [(OCT + UK) / 2] × 100 was used to compare mean FA values. The average difference was 0.00±0.11, the

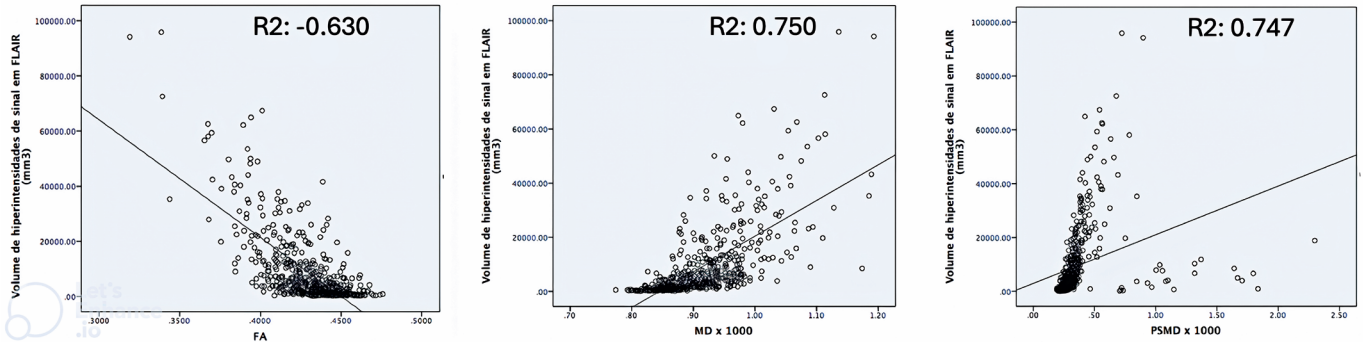

Figure 1. Relationship between the volume of white matter hyperintensities on FLAIR and the overall values of fractional anisotropy, mean diffusivity, and peak width of skeletonized mean diffusivity

Table 3. Interaction intensity values from the multivariate analysis of fractional anisotropy in white matter tracts corrected for sex, age, and education, distributed by regions of interest in the OCTAGENE study

MMSE FA			3MS FA		
FAanteriorthalamicradiationL	11,047	-0,67971633	FAanteriorthalamicradiationL	46,816	-0,794292026
anteriorthalamicradiationR	15,014	-0,47209065	anteriorthalamicradiationR	64,747	-0,563306528
corticospinaltractL	7,828	-0,84819302	corticospinaltractL	47,745	-0,782324734
corticospinaltractR	13,727	-0,53944993	corticospinaltractR	86,032	-0,28911511
forcepsmajor	25,384	0,070656583	forcepsmajor	108,764	0,003716431
forcepsminor	27,01	0,155758512	forcepsminor	93,531	-0,192513679
inferiorfrontooccipitalfasciculusL	8,552	-0,81030016	inferiorfrontooccipitalfasciculusL	36,521	-0,926911273
inferiorfrontooccipitalfasciculusR	46,287	1,164682176	inferiorfrontooccipitalfasciculusR	163,738	0,711886459
superiorlongitudinalfasciculusL	32,141	0,424305864	superiorlongitudinalfasciculusL	134,002	0,328830033
superiorlongitudinalfasciculusR	62,247	2	superiorlongitudinalfasciculusR	263,732	2
anteriorcoronaradiataL	4,634	-1,01536126	anteriorcoronaradiataL	21,864	-1,115721403
anteriorcoronaradiataR	9,76	-0,7470756	anteriorcoronaradiataR	33,029	-0,971894897
anteriorlimbofinternalcapsuleL	16,17	-0,41158768	anteriorlimbofinternalcapsuleL	57,825	-0,652475098
anteriorlimbofinternalcapsuleR	33,953	0,5191427	anteriorlimbofinternalcapsuleR	119,399	0,140715526
bodyofcorpuscallosum	4,717	-1,01101719	bodyofcorpuscallosum	17,708	-1,169258614
cerebralpeduncleL	37,574	0,708659357	cerebralpeduncleL	133,637	0,324128136
cerebralpeduncleR	26,711	0,140109387	cerebralpeduncleR	113,358	0,062895917
cingulumcingulategyrusL	42,044	0,942611153	cingulumcingulategyrusL	152,555	0,567828078
cingulumcingulategyrusR	47,598	1,233297569	cingulumcingulategyrusR	176,786	0,879969599
cingulumhippocampusL	-0,531	-1,28568812	cingulumhippocampusL	0,297	-1,39354552
cingullumhippocampusR	8,273	-0,82490252	cingullumhippocampusR	50,984	-0,740600233
externalcapsuleL	-3,836	-1,4586659	externalcapsuleL	-11,613	-1,546969048
externalcapsuleR	13,587	-0,54677727	externalcapsuleR	70,43	-0,490098643
fornixcresstriaterminalisL	23,76	-0,01434067	fornixcresstriaterminalisL	94,493	-0,180121283
fornixcresstriaterminalisR	15,543	-0,44440374	fornixcresstriaterminalisR	51,917	-0,728581412
fornixcolumnandbodyoffornix	33,976	0,520346479	fornixcolumnandbodyoffornix	131,275	0,293701069
genuofcospuscallosum	8,877	-0,79329024	genuofcospuscallosum	37,984	-0,908065041
pontinecrossingtract	-11,148	-1,84136289	pontinecrossingtract	-38,309	-1,890864473
posteriorcoronaradiataL	2,591	-1,12228823	posteriorcoronaradiataL	13,245	-1,226750571
posteriorcoronaradiataR	10,485	-0,7091304	posteriorcoronaradiataR	40,668	-0,873489999
posteriorlimbofinternalcapsuleL	-5,355	-1,53816764	posteriorlimbofinternalcapsuleL	-22,863	-1,691890517
posteriorlimbofinternalcapsuleR	-9,77	-1,76924083	posteriorlimbofinternalcapsuleR	-23,337	-1,697996541
posteriorthalamicradiationincludeopticradiationL	34,33	0,538874205	posteriorthalamicradiationincludeopticradiationL	121,574	0,168733676
posteriorthalamicradiationincludeopticradiationR	40,211	0,846675215	posteriorthalamicradiationincludeopticradiationR	144,399	0,462763234
retrolenticularpartofinternalcapsuleL	4,297	-1,03299924	retrolenticularpartofinternalcapsuleL	20,072	-1,138805783
retrolenticularpartofinternalcapsuleR	-14,179	-2	retrolenticularpartofinternalcapsuleR	-46,781	-2
sagittalstratumL	35,082	0,578232539	sagittalstratumL	134,427	0,334304844
sagittalstratumR	46,893	1,196399131	sagittalstratumR	157,893	0,636591705
spleniuofcorpuscallosum	-1,14	-1,31756209	spleniuofcorpuscallosum	6,124	-1,31848264
superiorcerebellarpeduncleL	24,009	-0,00130846	superiorcerebellarpeduncleL	79,211	-0,376982606
superiorcerebellarpeduncleR	11,134	-0,6751629	superiorcerebellarpeduncleR	36,051	-0,93296577
superiorcoronaradiataL	3,481	-1,07570722	superiorcoronaradiataL	20,576	-1,132313301
superiorcoronaradiataR	-0,241	-1,27051004	superiorcoronaradiataR	15,154	-1,202159008
posteriorthalamicradiationincludeopticradiationL_A	13,092	-0,57268469	posteriorthalamicradiationincludeopticradiationL_A	48,475	-0,772920941
posteriorthalamicradiationincludeopticradiationR_A	40,211	0,846675215	posteriorthalamicradiationincludeopticradiationR_A	144,399	0,462763234
superiorlongitudinalfasciculusL_A	29,082	0,264203282	superiorlongitudinalfasciculusL_A	94,726	-0,177119799
superiorlongitudinalfasciculusR_A	22,546	-0,07787926	superiorlongitudinalfasciculusR_A	91,989	-0,212377582
uncinatefasciculusL	17,485	-0,34276293	uncinatefasciculusL	74,326	-0,439910728
uncinatefasciculusR	27,133	0,162196111	uncinatefasciculusR	108,362	-0,001462097

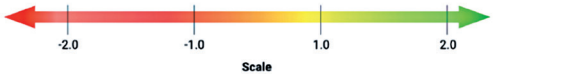

Created with the BioRender tool.. Available from: https://biorender.com
FA: fractional anisotropy.

Table 4. Interaction intensity values from the multivariate analysis of mean diffusivity in white matter tracts corrected for sex, age, and education, distributed by regions of interest in the OCTAGENE study

MMSE MD	beta	interaction	3MS MD	beta	interaction
FAanteriorthalamicradiationL	-19,487	-1,14868	MDanteriorthalamicradiationL	-71,008	-0,95655
anteriorthalamicradiationR	-15,854	-0,88197	anteriorthalamicradiationR	-54,285	-0,6159
corticospinaltractL	-21,124	-1,26886	corticospinaltractL	-64,571	-0,82543
corticospinaltractR	-10,062	-0,45675	corticospinaltractR	-10,128	0,28361
forcepsmajor	-3,575	0,019492	forcepsmajor	-4,369	0,400925
forcepsminor	-11,25	-0,54397	forcepsminor	-45,523	-0,43741
inferiorfrontooccipitalfasciculusL	-20,075	-1,19185	inferiorfrontooccipitalfasciculusL	-71,238	-0,96124
inferiorfrontooccipitalfasciculusR	4,234	0,592787	inferiorfrontooccipitalfasciculusR	7,261	0,637835
superiorlongitudinalfasciculusL	-4,371	-0,03895	superiorlongitudinalfasciculusL	-10,479	0,27646
superiorlongitudinalfasciculusR	15,591	1,426558	superiorlongitudinalfasciculusR	74,13	2
anteriorcoronaradiataL	-15,498	-0,85583	anteriorcoronaradiataL	-54,561	-0,62152
anteriorcoronaradiataR	-13,719	-0,72523	anteriorcoronaradiataR	-53,767	-0,60534
anteriorlimbofinternalcapsuleL	-9,235	-0,39604	anteriorlimbofinternalcapsuleL	-32,731	-0,17683
anteriorlimbofinternalcapsuleR	6,718	0,775149	anteriorlimbofinternalcapsuleR	23,76	0,973931
bodyofcorpuscallosum	-15,76	-0,87507	bodyofcorpuscallosum	-62,107	-0,77524
cerebralpeduncleL	9,211	0,958172	cerebralpeduncleL	39,518	1,294931
cerebralpeduncleR	2,992	0,501606	cerebralpeduncleR	27,124	1,042458
cingulumcingulategyrusL	1,413	0,385684	cingulumcingulategyrusL	0,8	0,506221
cingulumcingulategyrusR	1,107	0,363219	cingulumcingulategyrusR	2,893	0,548856
cingulumhippocampusL	-5,715	-0,13762	cingulumhippocampusL	-15,083	0,182674
cingullumhippocampusR	-19,845	-1,17497	cingullumhippocampusR	-65,701	-0,84845
externalcapsuleL	-13,91	-0,73925	externalcapsuleL	-49,426	-0,51692
externalcapsuleR	-6,308	-0,18115	externalcapsuleR	-16,153	0,160877
fornixcresstriaterminalisL	-16,1	-0,90003	fornixcresstriaterminalisL	-58,16	-0,69483
fornixcresstriaterminalisR	-17,623	-1,01184	fornixcresstriaterminalisR	-65,852	-0,85152
fornixcolumnandbodyoffornix	-0,579	0,239442	fornixcolumnandbodyoffornix	-2,455	0,439914
genuofcospuscallosum	-16,871	-0,95663	genuofcospuscallosum	-60,534	-0,74319
pontinecrossingtract	-6,411	-0,18871	pontinecrossingtract	-23,071	0,019953
posteriorcoronaradiataL	-10,451	-0,48531	posteriorcoronaradiataL	-35,565	-0,23456
posteriorcoronaradiataR	-3,273	0,041663	posteriorcoronaradiataR	-13,287	0,219259
posteriorlimbofinternalcapsuleL	-27,614	-1,74532	posteriorlimbofinternalcapsuleL	-102,043	-1,58876
posteriorlimbofinternalcapsuleR	-22,191	-1,3472	posteriorlimbofinternalcapsuleR	-63,807	-0,80987
posteriorthalamicradiationincludeopticradiationL	13,396	1,265412	posteriorthalamicradiationincludeopticradiationL	47,949	1,466676
posteriorthalamicradiationincludeopticradiationR	16,38	1,484482	posteriorthalamicradiationincludeopticradiationR	53,047	1,570526
retrolenticularpartofinternalcapsuleL	-6,141	-0,16889	retrolenticularpartofinternalcapsuleL	-14,885	0,186707
retrolenticularpartofinternalcapsuleR	-30,204	-1,93547	retrolenticularpartofinternalcapsuleR	-107,787	-1,70577
sagittalstratumL	14,448	1,342645	sagittalstratumL	56,041	1,631515
sagittalstratumR	23,402	2	sagittalstratumR	72,595	1,968731
spleniuofcorpuscallosum	-31,083	-2	spleniuofcorpuscallosum	-122,231	-2
superiorcerebellarpeduncleL	8,56	0,910379	superiorcerebellarpeduncleL	25,937	1,018278
superiorcerebellarpeduncleR	1,413	0,385684	superiorcerebellarpeduncleR	8,9	0,671223
superiorcoronaradiataL	-16,937	-0,96148	superiorcoronaradiataL	-59,559	-0,72333
superiorcoronaradiataR	-14,05	-0,74953	superiorcoronaradiataR	-41,715	-0,35984
uncinatefasciculusL	-12,227	-0,61569	uncinatefasciculusL	-41,451	-0,35446
uncinatefasciculusR	-6,63	-0,20479	uncinatefasciculusR	-25,939	-0,03847

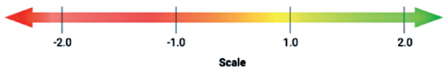

Created with the BioRender tool.. Available from: https://biorender.com

maximum (-29.46%) was in the left cingulate gyrus, and the smallest (-0.01%) was in the right hippocampus (Table 6).

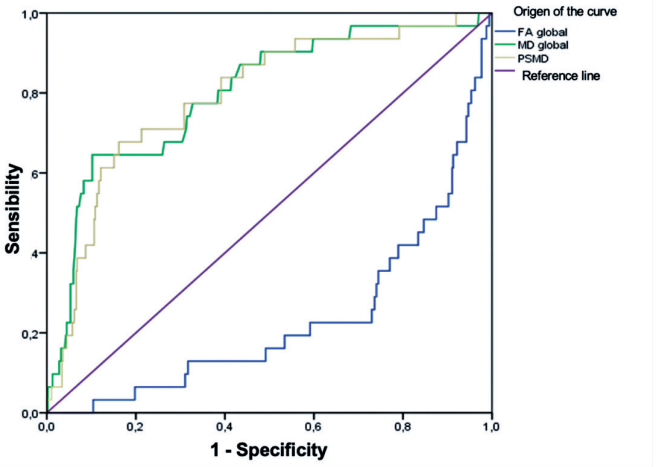

Figure 2. ROC curve for the outcome of MMSE ≤17

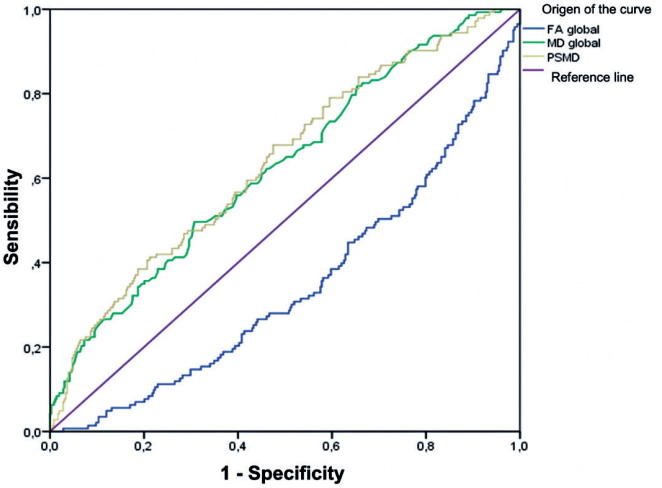

Figure 3. ROC Curve for the outcome of MMSE ≤23

Table 5. Distribution of mean ages after adjustment for the minimum age of 60 and maximum of 75 in the OCTAGENE and UK Biobank studies

Group	Total	Mean age	N [60-75 years old]	Mean age 60-75 years old sample	p value
OCTAGENE	504	74.7	282	67.6	<0.001
UK Biobank	40.521	62.9	21.932	65.7	<0.001
Total	41.025		22.214	63.3	

Student *t* test.
Demographic data: OCTAGENE and UKBiobank.

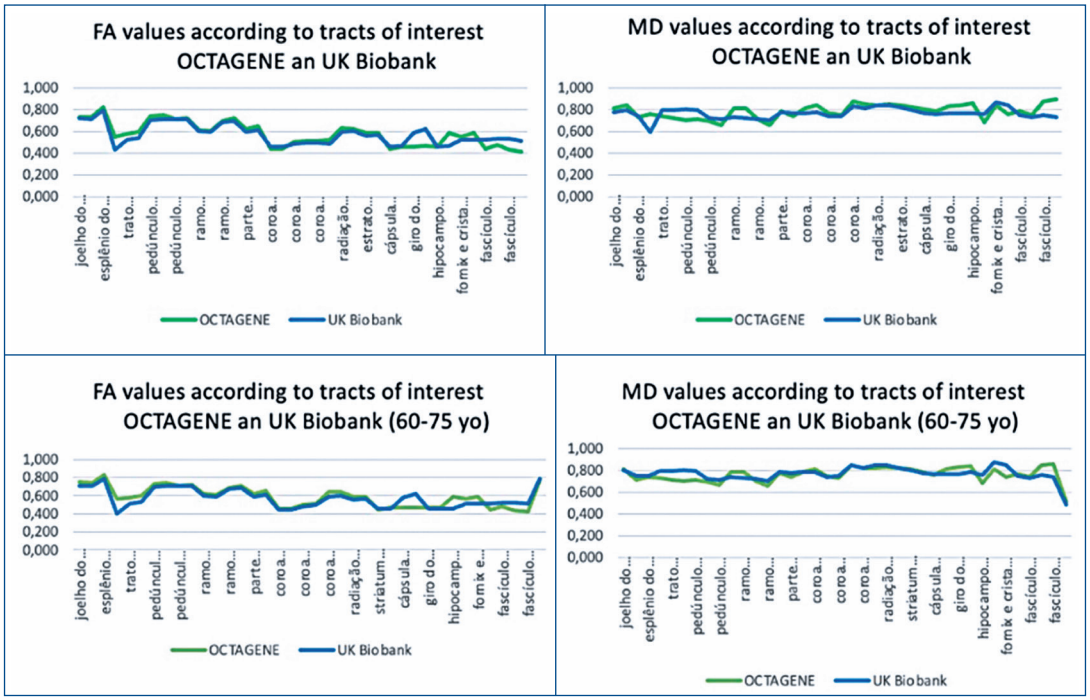

Figure 4. Distribution of mean fractional anisotropy and mean diffusivity values across different white matter tracts in the OCTAGENE and UK Biobank studies for complete sample and subsample individuals aged 60-75 years

Table 6. Mean FA values according to white matter tracts in OCTAGENE and UK Biobank samples and proportional difference formula (OCT − UK) / [(OCT + UK) / 2] × 100

FA	OCTAGENE	UKBiobank	OCT -UK / (OCT+UK/2)
Genu of cospus callosum	0,731	0,721	1,42
Body of corpus callosum	0,725	0,713	1,72
Spleniu of corpus callosum	0,823	0,788	4,34
Fornix column and body of fornix	0,547	0,430	23,99
Corticospinal tract Right	0,570	0,518	9,64
Corticospinal tract Left	0,592	0,538	9,59
Superior cerebellar peduncle Right	0,738	0,698	5,61
Superior cerebellar peduncle Left	0,746	0,708	5,23
Cerebral peduncle Right	0,708	0,708	0,07
Cerebral peduncle Left	0,717	0,712	0,67
Anterior limb of internal capsule Right	0,610	0,600	1,63
Anterior limb of internal capsule Left	0,600	0,590	1,62
Posterior limb of internal capsule Right	0,690	0,681	1,31
Posterior limb of internal capsule Left	0,715	0,688	3,90
Retrolenticular part of internalcapsule Right	0,619	0,594	4,05
Retrolenticular part of internal capsule Left	0,649	0,614	5,53
Anterior corona radiata Right	0,439	0,460	-4,63
Anterior corona radiata Left	0,439	0,452	-2,94
Superior corona radiata Right	0,497	0,483	2,93
Superior corona radiata Left	0,510	0,490	4,00
Posterior corona radiata Right	0,512	0,490	4,39
Posterior corona radiata Left	0,516	0,479	7,44
Posterior thalamic radiation include opticradiation Right	0,626	0,593	5,44
Posterior thalamic radiation include opticradiation Left	0,622	0,602	3,23
Sagittal stratum Right	0,583	0,560	4,07
Sagittal stratum Left	0,584	0,566	3,19
External capsule Right	0,437	0,457	-4,66
External capsule Left	0,456	0,466	-2,26
Cingulum cingulate gyrus Right	0,459	0,580	-23,23
Cingulum cingulate gyrus Left	0,462	0,622	-29,46
Cingullum hippocampus Right	0,459	0,459	-0,01
Cingulum hippocampus Left	0,587	0,462	23,84
Fornix cresstria terminalis Right	0,547	0,522	4,74
Fornix cresstria terminalis Left	0,583	0,523	10,73
Superior longitudinal fasciculus Right	0,442	0,520	-16,40
Superior longitudinal fasciculus Left	0,471	0,528	-11,49
Uncinate fasciculus Right	0,424	0,525	-21,24
Uncinate fasciculus Left	0,411	0,511	-21,66

Created with the BioRender tool.. Available from: https://biorender.com
FA: fractional anisotropy.

DISCUSSION

The traditional Fazekas scale revealed weaker correlations, with Spearman's rho coefficients ranging 0.417-0.414. This suggests that visual assessment methods may have inherent limitations compared to quantitative techniques, supporting the findings of van Straaaten et al.[27] who reported that, in a review of 618 independently living older adults, volumetric measures of white matter hyperintensities demonstrated greater sensitivity in detecting memory-related symptoms. This highlights the added value of objective metrics for evaluating cognitive health, particularly in aging populations.

Additionally, our results indicated a negative correlation between global FA and lesion burden, based on total lesion count and volume. This aligns with Andersen et al.'s findings that decreased FA values correlate with higher white matter lesion burden in patients with multiple sclerosis. Such associations imply that lower FA may reflect structural damage and serve as an important biomarker for ongoing neurodegeneration, contributing to cognitive decline.[28]

Furthermore, significant correlation was observed between the 3MS and MMSE cognitive assessments and diffusion metrics, with the FA showing positive correlations (Spearman's rho coefficients of 0.315 for 3MS and 0.285 for MMSE, $p<0.001$) and MD values displaying a negative correlation (Spearman's rho

coefficients of -0.237 for 3MS and -0.258 for MMSE). These findings align with those of Li et al.[29] who reported similar associations in a community-based cohort conducted on a rural population in China. Li et al. also observed global associations between FA and MD values and cognitive performance in the verbal fluency test. The consistent relationship between FA, MD, and various cognitive measures supports the role of white matter integrity in age-related cognitive decline.

This study showed that higher global FA scores correlate positively with higher 3MS and MMSE scores. This result aligns with previous research, including the findings of Xing et al., who, in an analysis of 77 participants with Fazekas 2 or 3, stratified by age, sex, education, and the presence of apolipoprotein E gene 4, identified mean global FA as the strongest risk marker for cognitive decline that exhibited statistical correlation with MMSE scores.[30]

Technological advances in the field now allow quicker image acquisition for DTI analysis with fewer artefacts, making clinical use of such techniques more feasible. Although some MRI metrics still require offline image processing steps, standardized strategies can help mitigate practical limitations.

Notably, this study focuses on region-specific assessment, such as the superior longitudinal fasciculus - the brain's largest associative fiber bundle.[31] Similarly, Koshiyama et al.[32] found that FA values in the superior longitudinal fasciculus strongly correlated with memory and visuospatial ability in 583 healthy volunteers aged 18-68 (mean age of 30.8) years.

Finally, our findings on associations between cognitive test alterations and specific regions, including the inferior fronto-occipital fasciculus, cingulate gyrus, posterior thalamic radiation, and fornix, align with Deng et al.[33] Their study found that elevated heart rates were linked to diminished performance in fluid intelligence tasks, suggesting phycological factors may interact with the structural integrity of white matter, further complicating our understanding of cognitive decline.

CONCLUSION

A substantial correlation was observed between white matter hyperintensities, cognitive performance, and diffusion metrics (fractional anisotropy, mean diffusivity, and peak width of skeletonized mean diffusivity). Although Magnetic resonance imaging metric assessment requires offline image processing, standardized strategies can help mitigate practical limitations. This comprehensive neuroimaging study provides valuable insights into the complex interplay among brain structure, cognitive decline, and aging. The findings enhance neuroradiology by highlighting potential biomarkers of cognitive aging and emphasizing the importance of region-specific analyses and quantitative imaging techniques.

AUTHORS' CONTRIBUTION

Mariana Athaniel Silva Rodrigues: conceived and executed the presented idea, data processing, writing and revision. Thiago Pereira Rodrigues: results analysis, revision. Aurea Beatriz Martins Bach: data processing, revision. Artur José Marques Paulo: data processing. Michel Satya Nasvlasky: idealization and execution of OCTAGENE study, maintained OCTAGENE data anonymity. Yeda Aparecida de Oliveira Duarte and Mayana Zatz: SABE study idealization. Edson Amaro Junior: supervision of OCTAGENE study, conceived and planned the presented idea, supervised the project.

AUTHORS' INFORMATION

Rodrigues MA: http://orcid.org/0000-0001-7566-3632
Rodrigues TP: http://orcid.org/0000-0002-4643-5339
Bach AB: http://orcid.org/0000-0002-7378-0867
Paulo AJ: http://orcid.org/0000-0003-1623-0639
Nasvlasky MS: http://orcid.org/0000-0002-9068-1713
Duarte YA: http://orcid.org/0000-0003-3933-2179
Zatz M: http://orcid.org/0000-0003-3970-8025
Amaro Junior E: http://orcid.org/0000-0002-5889-1382

REFERENCES

1. Morley JE. An Overview of Cognitive Impairment. Clin Geriatr Med. 2018;34(4):505-13.
2. Gonzales MM, Garbarino VR, Pollet E, Palavicini JP, Kellogg DL Jr, Kraig E, et al. Biological aging processes underlying cognitive decline and neurodegenerative disease. J Clin Invest. 2022;132(10):e158453.
3. Kumar A, Sidhu J, Goyal A, Tsao JW. Alzheimer Disease. StatPearls. Treasure Island (FL): StatPearls Publishing Copyright © 2022.
4. GBD 2016 Causes of Death Collaborators. Global, regional, and national age-sex specific mortality for 264 causes of death, 1980-2016: a systematic analysis for the Global Burden of Disease Study 2016. Lancet. 2017;390(10100):1151-210. Erratum in: Lancet. 2017;390(10106):e38.
5. Oliveira D, Jun Otuyama L, Mabunda D, Mandlate F, Gonçalves-Pereira M, Xavier m, et al. reducing the Number of People with Dementia Through Primary Prevention in Mozambique, Brazil, and Portugal: an analysis of population-based data. J Alzheimers Dis. 2019;70(s1):S283-S291.
6. Nitrini R, Ferri CP. Burden of dementia in Brazil. Arq Neuropsiquiatr. 2020;78(12):755-6.
7. Gallegos M, Morgan ML, Cervigni M, Martino P, Murray J, Calandra M, et al. 45 Years of the mini-mental state examination (MMSE): A perspective from ibero-america. Dement Neuropsychol. 2022;16(4):384-7.

8. Terribilli D, Schaufelberger MS, Duran FL, Zanetti MV, Curiati PK, Menezes PR, et al. Age-related gray matter volume changes in the brain during non-elderly adulthood. Neurobiol Aging. 2011;32(2):354-68.
9. Maj E, Jamroży M, Bielecki M, Bartoszek M, Gołębiowski M, Wojtaszek M, et al. Role of DTI-MRI parameters in diagnosis of ALS: useful biomarkers for daily practice? Tertiary centre experience and literature review. Neurol Neurochir Pol. 2022;56(6):490-8. Review.
10. Ranzenberger LR, Snyder T. Diffusion Tensor Imaging. StatPearls. Treasure Island (FL): StatPearls Publishing. Copyright © 2022, StatPearls Publishing LLC; 2022.
11. Grech-Sollars M, Hales PW, Miyazaki K, Raschke F, Rodriguez D, Wilson M, et al. Multi-centre reproducibility of diffusion MRI parameters for clinical sequences in the brain. NMR Biomed. 2015;28(4):468-85.
12. Zanon Zotin MC, Yilmaz P, Sveikata L, Schoemaker D, van Veluw SJ, Etherton MR, et al. Peak width of skeletonized mean diffusivity: a neuroimaging marker for white matter injury. Radiology. 2023;306(3):e212780.
13. Campaña Perilla LA, Mahecha Carvajal ME, Cardona Ortegón JD, Barragán Corrales C, Barrera Patiño AM. Diffusion tensor imaging protocol: the need for standardization of measures. Radiology. 2023;308(2):e230470.
14. Naslavsky MS, Scliar MO, Yamamoto GL, Wang JY, Zverinova S, Karp T, et al. Whole-genome sequencing of 1,171 elderly admixed individuals from São Paulo, Brazil. Nat Commun. 2022;13(1):1004.
15. Lebrão ML, Duarte YA, Santos JL, Silva NN. 10 Years of SABE Study: background, methodology and organization of the study. Rev Bras Epidemiol. 2019;21(Suppl 2):e180002.
16. Rodrigues MA, Rodrigues TP, Zatz M, Lebrão ML, Duarte YA, Naslavsky MS, et al. Quantitative evaluation of brain volume among elderly individuals in São Paulo, Brazil: a population-based study. Radiol Bras. 2019;52(5):293-8.
17. Fazekas F, Chawluk JB, Alavi A, Hurtig HI, Zimmerman RA. MR signal abnormalities at 1.5 T in Alzheimer's dementia and normal aging. AJR Am J Roentgenol. 1987;149(2):351-6.
18. Ribaldi F, Altomare D, Jovicich J, Ferrari C, Picco A, Pizzini FB, et al. Accuracy and reproducibility of automated white matter hyperintensities segmentation with lesion segmentation tool: A European multi-site 3T study. Magn Reson Imaging. 2021;76:108-15.
19. Fischl B. FreeSurfer. Neuroimage. 2012;62(2):774-81.
20. Arevalo-Rodriguez I, Smailagic N, Roqué-Figuls M, Ciapponi A, Sanchez-Perez E, Giannakou A, et al. Mini-Mental State Examination (MMSE) for the early detection of dementia in people with mild cognitive impairment (MCI). Cochrane Database Syst Rev. 2021;7(7):CD010783.
21. Tombaugh TN. Test-retest reliable coefficients and 5-year change scores for the MMSE and 3MS. Arch Clin Neuropsychol. 2005;20(4):485-503.
22. Jenkinson M, Beckmann CF, Behrens TE, Woolrich MW, Smith SM. FSL. Neuroimage. 2012;62(2):782-90. Review.
23. Baykara E, Gesierich B, Adam R, Tuladhar AM, Biesbroek JM, Koek HL, Ropele S, Jouvent E; Alzheimer's Disease Neuroimaging Initiative; Chabriat H, Ertl-Wagner B, Ewers M, Schmidt R, de Leeuw FE, Biessels GJ, Dichgans M, Duering M. A novel imaging marker for small vessel disease based on skeletonization of white matter tracts and diffusion histograms. Ann Neurol. 2016;80(4):581-92.
24. Cohen J. A power primer. Psychol Bull. 1992;112(1):155-9.
25. Kochhann R, Varela JS, Lisboa CS, Chaves ML. The Mini Mental State Examination: review of cutoff points adjusted for schooling in a large Southern Brazilian sample. Dement Neuropsychol. 2010;4(1):35-41.
26. Monroe T, Carter M. Using the Folstein Mini Mental State Exam (MMSE) to explore methodological issues in cognitive aging research [editorial]. Eur J Ageing. 2012;9(3):265-74.
27. van Straaten EC, Fazekas F, Rostrup E, Scheltens P, Schmidt R, Pantoni L, Inzitari D, Waldemar G, Erkinjuntti T, Mäntylä R, Wahlund LO, Barkhof F; LADIS Group. Impact of white matter hyperintensities scoring method on correlations with clinical data: the LADIS study. Stroke. 2006;37(3):836-40.
28. Andersen KW, Lasič S, Lundell H, Nilsson M, Topgaard D, Sellebjerg F, et al. Disentangling white-matter damage from physiological fibre orientation dispersion in multiple sclerosis. Brain Commun. 2020;2(2):fcaa077.
29. Li WX, Yuan J, Han F, Zhou LX, Ni J, Yao M, et al. White matter and gray matter changes related to cognition in community populations. Front Aging Neurosci. 2023;15:1065245.
30. Xing Y, Yang J, Zhou A, Wang F, Wei C, Tang Y, et al. White matter fractional anisotropy is a superior predictor for cognitive impairment than brain volumes in older adults with confluent white matter hyperintensities. Front Psychiatry. 2021;12:633811.
31. Janelle F, Iorio-Morin C, D'amour S, Fortin D. Superior longitudinal fasciculus: a review of the anatomical descriptions with functional correlates. Front Neurol. 2022;13:794618.
32. Koshiyama D, Fukunaga M, Okada N, Morita K, Nemoto K, Yamashita F, et al. Association between the superior longitudinal fasciculus and perceptual organization and working memory: A diffusion tensor imaging study. Neurosci Lett. 2020;738:135349.
33. Deng YT, Kuo K, Wu BS, Ou YN, Yang L, Zhang YR, et al. Associations of resting heart rate with incident dementia, cognition, and brain structure: a prospective cohort study of UKbiobank. Alzheimers Res Ther. 2022;14(1):147.